Power Conversion Efficiency Characterization and Optimization for Smartphones

Woojoo Lee[†] Yanzhi Wang[†], Donghwa Shin[‡], Naehyuck Chang[‡], and Massoud Pedram[†]

[†]University of Southern California, CA, USA, [‡]Seoul National University, Korea,

[†]{woojoole, yanzhiwa, pedram}@usc.edu, [‡]{dhshin, naehyuck}@elpl.snu.ac.kr

ABSTRACT

Modern smartphones consume significant power and can hardly provide a full day's use between charging operations even with a 2000 mAh battery. This is in spite of many power management techniques being employed in the smart phones. This paper starts from the observation that modern smartphones waste a significant amount of the battery's stored energy during power conversion from the 3.7V output of a Li-Ion battery cell to different voltage levels needed to power various modules in a smartphone (processors, memory, display, GPS, etc.) Indeed the power conversion efficiency from the battery source to point of use in the smart phone has on average of only 60-75% efficiency. The approach taken to reduce this energy waste in smartphones is to (i) profile the power consumption of each module under different operating scenarios, (ii) build an equivalent DC-DC converter model for each smartphone module and estimate its power conversion efficiency, and (iii) change the parameters of the actual converters in the smartphone to improve the equivalent power conversion efficiencies for all modules. Experimental results demonstrate that we can achieve 6% to 15% power conversion efficiency enhancement, which translates to up to 30% reduction in the power losses incurred during power conversion in smartphones.

Categories and Subject Descriptors

C.5.3 [**Computer system implementation**]: Microcomputers

Keywords

Portable device, Smartphone, DC-DC converter, Power tree

1. INTRODUCTION

Modern smartphones are typically equipped with a multi-core gigahertz processor, gigabytes of high-speed DDR SDRAM, dozens of gigabytes of flash memory, several up to 10 megapixel cameras, 1M+ pixel high-resolution color display, high-power audio, as well as 3G/4G, Wi-Fi and Bluetooth wireless communication devices. Consequently, their power consumption is as high as a small-size notebook computer or a tablet. Although the smartphone battery capacity has been increased from several hundred mAh to over 2000 mAh over the last few years, the actual battery life (i.e., the service time between consecutive charges) has become
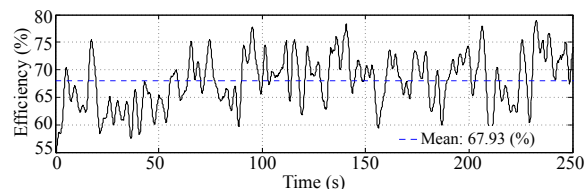
Figure 1: Measured of traces of power conversion efficiency of Qualcomm Snapdragon MDP MSM8660.

shorter due to even faster increase in the power consumption of the smartphones. An examination of the technology trends reveals that smartphone system-on-chips are migrating from dual cores to quad cores, display sizes continue to increase with some high-end smartphones having over 5" display, wireless data communication rates are increasing rapidly with a100MHz aggregated bandwidth, 4G LTE-Advanced providing almost 3.3Gbit peak download rates per sector of the base station, and so on. All this will result in significantly higher power consumption in the smartphones and a smaller battery life (active users of a recent 4G smartphone claim less than 2-3 hours of battery life.) High power consumption of smartphones (and relatively slow rate of increase in the energy storage density of batteries) is thus a serious concern that could derail the smartphone technology development and adoption.

It is not surprising that system-level power optimization and management have been widely investigated and advanced over the last two decades. Some recent works have explicitly focused on smartphones. In particular, references [1, 2, 3, 4] have presented various power dissipation models for the smartphones. Dynamic voltage (and frequency) scaling techniques have also been used to reduce the power consumption of various smartphone modules, including the CPU [5] and the display [6]. LCD backlight scaling has also been widely investigated [7].

Power optimization and management works for smartphones have targeted power savings in embedded processors, memory, display, and so on. None has addressed the issue of power conversion efficiency in the smartphones. This is an important problem that has gone unnoticed. More precisely, modern smartphones are equipped with many modules, each requiring its own supply voltage level which is typically different from those of other modules in the system. The smartphone is powered by a secondary (rechargeable) Li-Ion battery comprised of a single battery cell providing an initial output voltage level of 4.2V for a fully charged cell and as low as 3.0V for a nearly discharged battery (this yields the familiar nominal average output voltage level of 3.6 or 3.7V at 0.5C discharge rate.) This cell output voltage must be converted and regulated to different pre-determined voltage levels and distributed to various modules in the smartphone.

We have performed extensive measurement of power conversion efficiency for Qualcomm's smartphone platform, MDP MSM8660, as shown in Figure 1. Surprisingly, the power conversion efficiency of MDP MSM8660 ranges just from below 60% to slightly over 75%. Improving the power conversion efficiency can achieve significantly longer battery life. This paper thus focuses on power con-

version efficiency in smartphones and introduces power conversion efficiency characterization and optimization procedures.

Modern DC-DC converters exhibit very high peak conversion efficiency, but their conversion efficiency can drop dramatically due to the operating conditions, i.e., their output current level [8]. In other words, a low overall conversion efficiency of DC-DC converters is mainly due to mismatch between the power converter characteristics and the load demands.

In this paper we propose a general *equivalent DC-DC converter model* to model different types of converters (such as a buck DC-DC converter, a boost DC-DC converter, low-dropout (LDO) converter) and their series combinations in a power delivery path from the battery cell to the load device. In particular, we use the DC-DC converter model from [8] and identify coefficients of the equivalent power converter models with the aid of the application profiling tool named Trepn™.

We propose device grouping to enhance the accuracy of linear regression used for power efficiency characterization of the equivalent DC-DC converter. We then verify the accuracy of the power conversion efficiency characterization with real measurements. The results point to the fact that power conversion efficiency of the smartphone platform is quite low. Next, we model and verify the current demand distribution for each module in the smartphone platform and derive its expected value. Finally, we adjust the DC-DC converter parameters to ensure that the power converters operate at the most efficient points. Experimental results demonstrate that we can achieve 6% to 15% power conversion efficiency enhancement, which translates to up to 30% reduction in the power losses incurred during power conversion in smartphones.

Notice that the proposed flow can be exploited to do optimization in presently available commercial smartphone platforms, which do not have current sensors to report the component current demands under different applications and usage scenarios. This is possible because we make use of activity profiling-based power estimation [1, 2, 3, 4].

2. POWER CONVERSION LOSS MODELS

Given that the smartphones integrate hardware modules that have their own supply power lines and require their own voltages, it is necessary to generate different voltages for various modules from a single battery that powers the smartphone. A power conversion tree, with the root of the tree being the battery cell, the leaf nodes being the modules, and the internal nodes being DC-DC converters, is designed to achieve this goal. A conceptual example of the power conversion tree for a smartphone is depicted in Figure 2.

Typical DC-DC converters in modern smartphones can be classified into two types, switching-mode DC-DC converters (simply called DC-DC converter) and low-dropout linear regulators (LDO), according to the circuit implementation and operation principles. A DC-DC converter consists of an inductor, capacitors, two MOSFET switches and a pulse-width-modulation (PWM) controller. This type of converter can step-up the output voltage so that it becomes higher than the input voltage (i.e., boost), or step-down the output voltage so that it is lower than the input voltage (i.e., buck). On the other hand, the output voltage of an LDO can only be lower than its input voltage. In general, the LDO has lower power conversion efficiency. Nevertheless, the LDO is an indispensable component in smartphones in that it can provide low-noise output voltage, and therefore, the LDO is the most suitable type of converter to provide power for some noise-sensitive RF or analog modules.

2.1 DC-DC converter power loss model

The power loss model of a PWM DC-DC converter is well-studied in [8]. In general, the major sources of power loss in a DC-DC converter are conduction loss, switching loss in the power switches, and controller power loss, denoted by $P_{conduction}$, $P_{switching}$, and $P_{controller}$, respectively. The power loss of the buck converter,
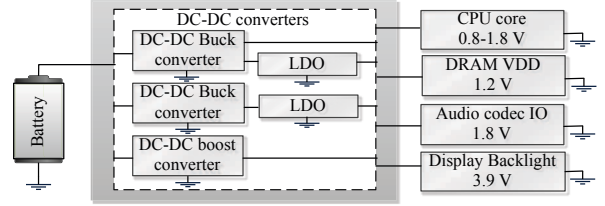
Figure 2: Conceptual diagram of a smartphone power conversion tree.

P_{buck}, can be expressed as:

$$P_{buck} = P_{conduction} + P_{switching} + P_{controller} \qquad (1)$$

$$= I_{out}^2 (R_L + DR_{sw1} + (1-D)R_{sw2}) \qquad (2)$$
$$+ (\Delta I)^2 (R_L + DR_{sw1} + (1-D)R_{sw2} + R_C)/12$$
$$+ V_{in}f_s(Q_{sw1} + Q_{sw2}) + V_{in}I_{controller},$$

where $D = V_{out}/V_{in}$ is the PWM duty ratio of the power switch, and V_{in} and V_{out} denote the input and output voltages, respectively; I_{out} is the output current through the inductor; $\Delta I = (1-D)V_{out}/(L_f f_s)$ is the amplitude of the maximum current ripple at the inductor; f_s is the switching frequency; and $I_{controller}$ denotes the current used in the control logic section of the converter. Series resistances of the inductor L and capacitor C are denoted by R_L and R_C, respectively. Similarly, series resistances of the two MOSFET switches are represented by R_{sw1} and R_{sw2}, respectively, while the amounts of their gate charge are denoted by Q_{sw1} and Q_{sw2}, respectively. The first and second terms of (2) are DC and AC conduction losses, respectively; third term of (2) denotes the switching loss; while the last term of (2) corresponds to the controller power loss.

The power loss of the boost converter, P_{boost}, is modeled similarly except for the switching duty calculation, which is given by:

$$P_{boost} = \left(\frac{I_{out}}{1-D}\right)^2 (R_L + DR_{sw1} + (1-D)R_{sw2} + D(1-D)R_C)$$
$$+ \frac{(\Delta I)^2}{12}(R_L + DR_{sw1} + (1-D)R_{sw2} + (1-D)R_C)$$
$$+ V_{in}f_s(Q_{sw1} + Q_{sw2}) + V_{in}I_{controller}, \qquad (3)$$

where $D = 1 - V_{in}/V_{out}$ and $\Delta I = (V_{in}D)/(L_f f_s)$.

As a result, the efficiency of a DC-DC converter, $\eta_{switching}$, can be calculated as:

$$\eta_{switching} = \frac{V_{out}I_{out}}{V_{in}I_{in}} = \frac{V_{in}I_{in} - P_{converter}}{V_{in}I_{in}}, \qquad (4)$$

where I_{in} is the input current, and $P_{converter}$ is either P_{buck} or P_{boost} depending on the type of DC-DC converter used.

2.2 LDO power loss model

A typical LDO consists of an error amplifier, a pass transistor, and a feedback resistor network. The power loss of the LDO, denoted by P_{ldo}, is given by:

$$P_{ldo} = I_{out}(V_{in} - V_{ref}k) + I_qV_{in}, \qquad (5)$$

where V_{ref} is the reference voltage in the error amplifier; $k = (R_1 + R_2)/R_2$ corresponds to the voltage divider's gain coefficient, and I_q denotes the quiescent current of the LDO. Unlike the switching converter in which the MOSFET switches dominate the total power loss, the pass transistor in the LDO has negligible impact on its total power loss [8]. Therefore, the power loss due to internal resistance of the pass transistor is not accounted for in the model. Thus the conversion efficiency of the LDO, η_{ldo}, may be expressed as:

$$\eta_{ldo} = \frac{V_{out}I_{out}}{V_{in}I_{in}} = \frac{k\,V_{ref}I_{out}}{V_{in}(I_{out}+I_q)} \qquad (6)$$
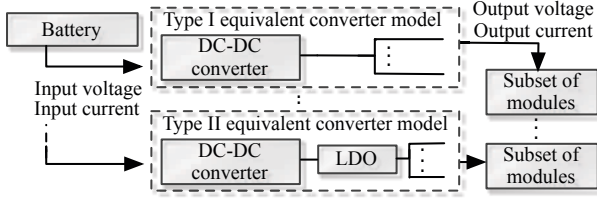
Figure 3: Types I and II equivalent power converter models.

3. CHARACTERIZATION OF THE POWER CONVERSION EFFICIENCY

Power converters including switching-mode DC-DC converters exhibit different conversion efficiency as a function of the load current [8]. A module is often powered through a set of converters from a battery source as shown in Figure 3. The power converter set can be an empty set (direct connection), single DC-DC converter, (more commonly) a cascade (series) connection of a DC-DC converter and an LDO, (rarely) a cascade connection of various DC-DC converters, etc. Characterization of each power converter efficiency is not a trivial work unless the power conversion tree structure and converter specifications, and all the node voltages and branch currents of the conversion tree are available. Such a *white-box* approach is generally not possible for commercial smartphones. Although the Qualcomm MDP provides measurement of the device current values, the power conversion tree structure is not available for examination/measurements.

In this paper, we attempt a *gray-box* approach introducing an *equivalent power converter* concept. The equivalent converter models a set of power converters from the battery source to each module. In other words, the proposed equivalent power converter abstraction treats the set of power converters as a single equivalent converter. The abstraction enables a gray-box approach by which one can group modules in a (smartphone) system by their required supply voltage levels, which can be obtained from datasheets. Power conversion efficiency improvement in the subsequent optimization procedure can be effectively performed once we identify the power conversion efficiency of all the power conversion paths from the battery source to various modules in the system.

3.1 Equivalent converter model

We classify the equivalent converter models either a single DC-DC converter, or a cascaded DC-DC converter and an LDO, named Type I and Type II equivalent converters, respectively. We assume that the battery output current goes through a voltage regulator in order to produce a constant voltage throughout its full discharge cycle. Without loss of generality, Types I and II equivalent converter models can represent most power conversion tree structures [9, 10, 11]. Most digital logic components can be powered by a single DC-DC converter from the battery to the module - this gives rise to Type I converter model. A cascade of two or more DC-DC converters are rare, because increasing the number of cascade DC-DC converters increases the cost and form factor overhead with little (or no) benefit in terms of conversion efficiency. LDOs are often an indispensable component to provide low-ripple output voltage for switching noise-sensitive RF and analog modules. It is uncommon to use a single LDO from the battery to a device due to large dropout voltage. Instead, the conversion of the battery voltage to an initially higher target voltage using a DC-DC converter and subsequent use of LDO for the final power conditioning is a more efficient way of doing this - hence, our emphasis on Type II converter model.

According to (2), (3), and (5), the power loss of the equivalent converter can be expressed as:

$$P_{eqv} = A(\alpha I_q + \sum_{i=1}^{N} I_{mod,i})^2 + \alpha\beta \sum_{i=1}^{N} I_{mod,i} + (B + \alpha\gamma I_q), \quad (7)$$

where N is the number of modules connected to the equivalent converter; $I_{mod,i}$ is the input current of the ith module; A is determined

Table 1: Grouping results for Snapdragon MDP MSM8660.

Group	Modules	Voltage
1 and 2	Group1: CPU core0 and Group2: CPU core1	0.8-1.225 V
3	Internal Memory, Audio DSP, and Digital core (includes GPU and modems)	1.1 V
4	Audio codec Vdd, LPDDR2 Vdd, ISM Vdd, DRAM Vdd2, and Camera digital	1.2 V
5	Audio codec IO , IO PAD3, Display IO, DRAM Vdd1, Camera IO, PLL, and eMMC host interface	1.8 V
6	Audio codec analog, Haptic, SD card, Touch screen, eMMC (Flash), IO PAD2, SD card, and Ambient light sensor	2.85 V
7	Display Memory and Display backlight	3.8 V

by the type of the DC-DC converter such that $A = R_L + DR_{sw1} + (1-D)R_{sw2}$ for buck converter and $A = (1/(1-D))^2(R_L + DR_{sw1} + (1-D)R_{sw2} + D(1-D)R_C)$ for boost converter; B is the sum of the second, third, and last terms of (2) or (3); $\alpha = 0$ for Type I, and $\alpha = 1$ for Type II; γ is the input voltages of the LDO; and $\beta = (\gamma - V_{ref}k)$. We can further simplify (7) by defining the output current of the equivalent converter, $I_{eqv\_out} = \sum_{i=1}^{N} I_{mod,i}$, and thus, the power loss for both types of equivalent converter models can be expressed as:

$$P_{eqv} = aI_{eqv\_out}^2 + bI_{eqv\_out} + c, \quad (8)$$

where the coefficients a, b, and c are derived from (7), and are largely dependent on the power converter design specification such as the power MOSFET gate width, inductor IR loss, controller loss, etc. [8]. Calculating those coefficients is the key step in of the power conversion efficiency characterization.

3.2 Power converter grouping and regression analysis

Measurement (or estimation) of the output current of all the equivalent power converters enables us to calculate the unknown coefficients of the equivalent power converter model. Once again, the input and output voltage levels of each equivalent power converters can be obtained from the device datasheets. The Qualcomm Snapdragon MDP MSM8660 [12] incorporates embedded power sensors that monitor and report current values of different modules with fine granularity. When the target smartphone does not provide embedded current sensors, we can estimate the module current values by activity profiling [1, 2, 3, 4].

Profiling various applications, which result in diverse usage patterns of the system modules, provides sufficient information and data to perform regression analysis and obtain the unknown coefficients. Linear regression analysis is a widely used method in system identification, requiring (i) a well-designed model and (ii) sufficient experimental data to extract the best-fit model coefficients. In reality, however, independent control of each module is a challenging task due to the lack of direct control knobs. For example, if we run an application that activates a camera module, the CPU, GPU, memory, and other associated component currents also ramp up and down. We must thus apply linear regression analysis to the whole system (including all smartphone modules) simultaneously, while trying to vary the activity level of each module by running different applications. However, this method may not produce sufficient data to cover the full range of activities for all smartphone modules, especially when the number of modules is large (e.g., the Snapdragon MDP MSM8660 has 27 embedded modules.) This is a potential source of inaccuracy for regression analysis due to the *weak training set* issue.

We tackle the problem by doing a module grouping in order to reduce the number of unknown coefficients that must be determined during the characterization process. This grouping procedure reduces the burden in terms of generating sufficient data for performing the linear regression analysis. The idea is that system modules that require the same operating voltage level can be combined into one group, and each group of modules is connected to the battery source via a single equivalent converter, as illustrated in Figure 3.

This method matches well with low power design practices that try to minimize the number of power converters, due to their cost and internal power losses.

Given that the number of different voltage levels required by various modules in a smartphone platform is typically less than 10 [9, 11], the grouping method significantly reduces the number of parameters to be determined in linear regression. For example, the Snapdragon MDP MSM8660 requires only seven groups although the module count is 27.

Finally, the total power loss of the smartphone, P_{loss}, is given by,

$$P_{loss} = \sum_{k=1}^{G} P_{eqv,k} = \sum_{k=1}^{G} (a_k I_{eqv\_out,k}^2 + b_k I_{eqv\_out,k} + c_k), \quad (9)$$

where G is the number of groups; $P_{eqv,k}$ is the power loss of the kth equivalent converter corresponding to the kth group of modules; $I_{eqv\_out,k}$ denote the output current of the equivalent converter, which can be measured using embedded sensors in the Snapdragon MDP MSM8660; a_k, b_k, and c_k are the coefficients of the equivalent converter model (to be determined by linear regression.) We treat the battery voltage presented to the power conversion tree as being (nearly) constant, which is valid considering the function of the regulator between the battery cell/pack and the equivalent converter, therefore, we may assume that a_k, b_k, and c_k are constant values.

3.3 Experimental results

3.3.1 Experimental setup

We use the Snapdragon MDP MSM8660 (in short, MDP) as a target platform. It is a cutting-edge smartphone platform equipped with Google Android OS 2.3 on top of Snapdragon 1.5 GHz asynchronous dual-core CPU, a 3D-supporting GPU, 3.61″ WVGA multi-touch screen, 1 GB internal RAM, 16 GB on-board flash, WiFi, Bluetooth, a GPS, dual-side cameras, etc. We perform power measurement of each module using the application profiling tool named Trepn™. Use of Trepn™ ensures higher accuracy of the measurements. Note, however, that our proposed method is independent of the measurement tools, e.g., we may use activity profiling for power measurement provided by Google or based on techniques presented in the literature [1, 2, 3, 4].

3.3.2 Coefficient identification

As shown in Table 1, the MDP modules may be classified into seven groups based on their operating voltage levels. Some modules such as the CPU cores in the MDP use dynamic voltage and frequency scaling (DVFS) techniques that require a range of variable supply voltage levels. Consequently, we keep each CPU core in a separate group but treat the equivalent converters of these groups identical to each other. Group 7 is associated with display, and therefore, the backlight luminance level mostly determines the current demand in this group. Group 7 coefficients are easy to identify because we can independently control the brightness of the display. In other words, we first perform the linear regression to identify coefficients of the equivalent converter model of Group 7, separately from the other groups.

For the remaining six groups, we profile various applications and collect sufficient data for the regression analysis as explained earlier. It is difficult to identify every c_k coefficient of the kth equivalent converters directly from the linear regression process. Rather, we only extract c_{ext} that corresponds to the sum of all the constant terms in (9), i.e., $c_{ext} = \sum_{k=1}^{G} c_k$. We find an approximate value for each c_k as $c_k = c_{ext}(P_{group,k}/P_{group,total})$, where $P_{group,k}$ denotes the power consumption of Group k, and $P_{group,total}$ is the total power consumption of all the groups. The $P_{group,k}$ and $P_{group,total}$ values are available from the embedded sensors in the MDP.

The extracted coefficients of the seven equivalent converters are reported in Table 2. The power conversion efficiency of Group k, derived from $(P_{group,k}/(P_{group,k} + P_{eqv,k}))$, is shown in Figure 4. We verify the characterization results of each equivalent power

Table 2: Extracted coefficients for each group.

| k	a_k	b_k	c_k	k	a_k	b_k	c_k
1, 2	0.4427	0.0025	0.0170	5	0.1971	0.5232	0.0128
3	0.4079	0.1742	0.0675	6	0.1814	0.2928	0.0320
4	0.1152	0.1757	0.0077	7	0.4091	0.3871	0.0289
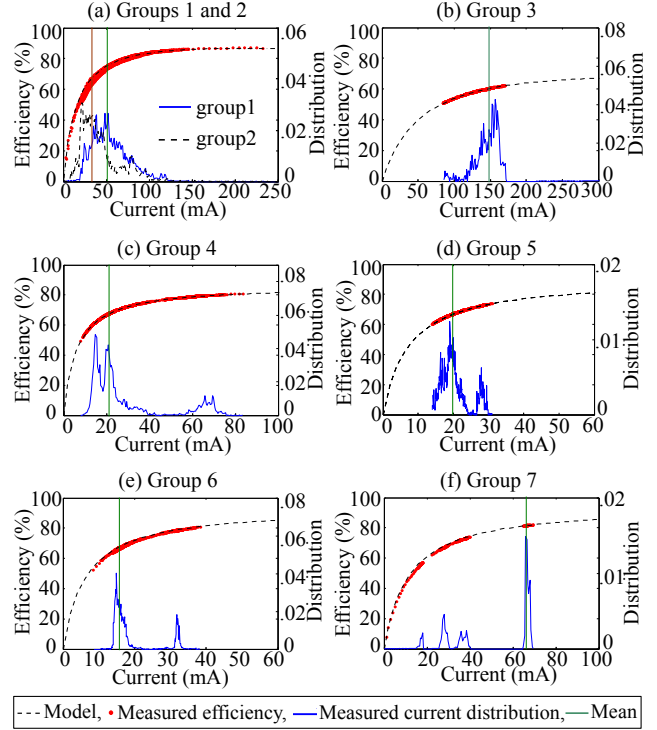
Figure 4: Conversion efficiencies for all groups.

converters. Figure 5 shows the comparison of the system power consumption trace between the real measurement as reported by a built-in battery sensor and the estimation as obtained by our extracted equivalent converter coefficients. We have thus confirmed that the results of the power conversion efficiency characterization process is accurate enough for the subsequent optimization process.
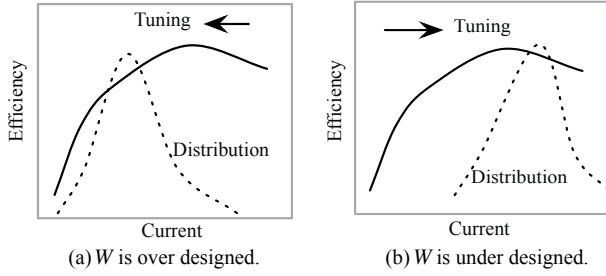
4. POWER CONVERTER TUNING

Power converter tuning reduces power loss without any performance degradation. This is because, unlike typical low-power design techniques that often exploit a tradeoff between performance/service quality and power efficiency, the power converter tuning does not utilize slack time of the system.

Enhancement of the overall efficiency of a DC-DC converter can greatly increase the overall system power efficiency [13, 9]. DC-DC converters show very high overall efficiency under the right operating conditions. However, their efficiency can be low if they are operated outside the recommended range on input and output voltages and load currents [8]. Therefore, ensuring that each DC-DC converter in the system is operating under the right operating conditions is an effective way of improving the system power efficiency. For example, Reference [10] presents a dynamic programing ap-
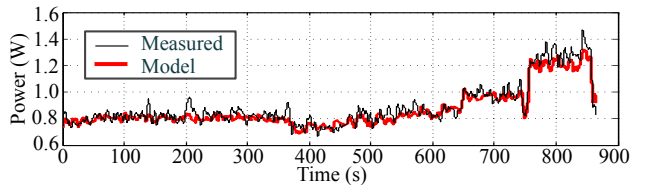
Figure 5: A part of traces of total power consumption: measured data and modeled data.

Figure 6: Concept of the width tuning.

(a) W is over designed. (b) W is under designed.

proach to design the structure of the power conversion tree in a system while at the same time selecting the 'optimal' DC-DC converter or LDO for each node of the conversion tree. Reference [14] proposes the concept of parallel connections of high frequency DC-DC converters for distributed energy storage systems. In contrast, the present paper starts with a fixed conversion tree structure, but uses load currents demands and converter characteristics to perform MOSFET switch sizing so as to improve the overall efficiency of the power conversion process in a smartphone system.

As stated above, we focus on the optimal assignment of the gate width, W, of the MOSFET switches in a DC-DC converter. The pass transistor in the LDO has negligible impact on its power loss, therefore, we do not take it into account. (c.f. Section 2.2.) As we previously depicted in Figure 4, DC-DC converters in the MDP are not properly tuned in regard to the actual Android applications running on it. The width tuning, which was introduced in [8], is conceptually explained in Figure 6. The idea is to match the value of W in the equivalent converter such that the desirable operating conditions of the equivalent converter match with the current distribution produced by the actual usage profiles of various Android applications in order to yield the maximum conversion efficiency for the typical daily use of a smartphone.

Sizing down W causes the turn-on resistance of the MOSFET increased and the gate charge decreased. (i.e., $W = (W_o R_o)/R_{sw1,2} = (W_o Q_{sw1,2})/Q_o$; R_o and Q_o correspond to the turn-on resistance and the gate charge of a MOSFET with a gate size of W_o, respectively.) As a function of W, we can express the DC-DC converter power loss models, (2) and (3), as:

$$P_{converter} = \left(\frac{r_1}{W} + r_2\right) I_{out}^2 + r_3 W + r_4, \quad (10)$$

where I_{out} denotes the output current of the DC-DC converter; r_1, r_2, r_3, and r_4 are constants.

Given that the two MOSFET switches in a DC-DC converter dominate the power loss of the equivalent converter, and I_q is small, we rewrite (8) as:

$$P_{eqv,k} = \left(\frac{r_{1,k}}{W_k} + r_{2,k}\right) I_{eqv\_out,k}^2 + bI_{eqv\_out,k} + r_{3,k}W_k + r_{4,k}, \quad (11)$$

where $P_{eqv,k}$ and $I_{eqv\_out,k}$ are the power loss and the output current of the kth equivalent converter, respectively, corresponding to the kth group of modules; W_k, $r_{1,k}$, $r_{2,k}$, $r_{3,k}$ and $r_{4,k}$ are the coefficients of the equivalent converter model that have been determined

(a) Efficiency : Group 7   (b) Power loss : Group 7
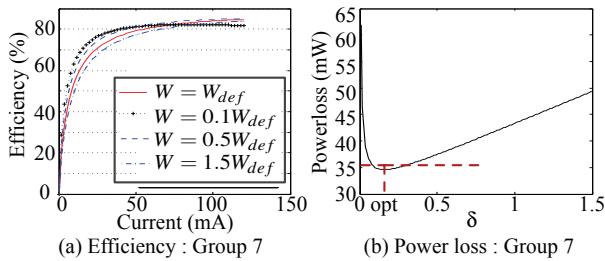
Figure 7: Relation between the power conversion efficiency and W: Group 7.

Table 3: W_{def} of the equivalent converter models.

Group	1 and 2	3	4	5	6	7
W_{def}	1.2401	1.1033	1.3109	1.4033	1.4102	0.7368

based on linear regression. The resultant coefficient W_k is the default value of W (W_{def}) of the kth equivalent converter, which is shown in Table 3.

4.1 Width tuning

Figure 7 (a) shows an example in which W changes the efficiency graph of Group 7. Note that the efficiency of the DC-DC converter increases as W becomes smaller (larger) in the relatively low (high) current demand region. Other groups show similar behaviors. Figure 7 (b) shows the relation between the power loss and W under the condition that the output current of Group 7 is 37 mA. Here, δ is a control variable such that the modified value of W is calculated as $\delta \cdot W_{def}$. The power loss plots have a convex functional form in terms of W, which implies that there is a globally optimal value of W, W_{opt}, that minimizes the power loss of the equivalent converter. Given that I_{eqv_out} is a random variable, our goal of finding W_{opt} for the actual usages of the various applications should be based on the probability distribution of I_{eqv_out} acquired by the usages of the applications. Such probability distribution can be obtained via real measurements, yielding the current profile of each module (thereby, each group of modules) when each type of application is running. We run 10 representative smartphone applications and collect the probability distribution of I_{eqv_out} for each group of modules and for each application.

Throughout the module current profiles collection and (11), the expected power loss of an equivalent converter can be generally expressed as:

$$E[P_{eqv}] = \left(\frac{r_1}{W} + r_2\right) E[I_{eqv\_out}^2] + bE[I_{eqv\_out}] + r_3 W + r_4. \quad (12)$$

where $E[I_{eqv\_out}]$ denotes the expected value of I_{eqv_out}, and $E[I_{eqv\_out}^2]$ is the expected value of $I_{eqv\_out}^2$.

To find W_{opt}, we limit δ to two decimal places to avoid high computation cost (also in practice, two decimal place precision is quite adequate.) We define the *power conversion efficiency enhancement* by $Gain_\eta = 100\left(\eta_{optimal}/\eta_{original} - 1\right)$ and *power loss reduction* by $Gain_P = 100(1 - P_{optimal}/P_{original})$, where the optimal power conversion efficiency, $\eta_{optimal}$, and power loss, $P_{optimal}$, are derived from (10) with the optimal value of δ, and the original power conversion efficiency, $\eta_{original}$, and power loss, $P_{original}$ are derived from (10) with $\delta = 1$.

4.2 DC-DC converter tuning results

Table 4 shows an example of the width tuning that each W_{opt} is derived from each group and four different applications, 'Clock', 'Call', 'Facebook', and 'Skype-videochat'. As each application causes different current distribution, the values of W_{opt} for the same group are different. Table 4 also shows the tuning results for the four applications. According to the resulted W_{opt} for each group, the $Gain_\eta$ and $Gain_P$ columns show the resultant gains for each group. The upper bound of the power conversion efficiency enhancement ($Gain_{\eta,max}$) and the power loss reduction ($Gain_{p,max}$) are obtained from the distribution of I_{eqv_out} and W_{opt}.

We collect the current distribution data from 10 applications, including the four applications named in Table 4, 'Camera', 'Google-Map', 'Neocore', 'SMS', 'System setting', and 'Youtube'. All the applications except 'Clock' and 'System setting' are run under the same setup where WiFi is turned on and the backlight level of the display is the highest. 'Clock' is measured under the median level of the backlight and WiFi on, whereas 'System setting' is measured under the lowest backlight and WiFi off. For the case of 'Call', we consider auto turn-off screen during the call. We, then, classify the 10 applications into seven categories, i) *communication* (contains 'SMS', 'Call', and 'Skype-videochat'), ii) *browsing* (contains 'Web browsing'), iii) *media* (contains 'Camera' and 'Youtube'),

Table 4: Example of DC-DC converter tuning results of four types of applications.

Group	Clock					Call				
	W_{opt}	$Gain_\eta$	$Gain_P$	$Gain_{\eta,max}$	$Gain_{P,max}$	W_{opt}	$Gain_\eta$	$Gain_P$	$Gain_{\eta,max}$	$Gain_{P,max}$
1	0.2356	11.3508	34.5181	27.2733	43.1362	0.2852	8.7073	30.6121	23.7710	40.8894
2	0.1369	21.1175	42.8718	31.2166	47.0092	0.1991	12.9707	37.3828	27.1296	44.5621
3	0.3751	6.7329	15.7217	13.5717	24.4609	0.3751	6.6543	15.5894	13.5717	24.4609
4	0.1180	15.2996	34.9625	19.4536	38.4971	0.1704	10.2327	28.7502	12.4670	31.7882
5	0.1123	15.5010	30.7496	17.9247	33.0915	0.1263	13.0017	27.9058	15.4971	30.7201
6	0.1128	14.6603	34.4909	15.9501	35.8211	0.1269	14.0235	33.7792	16.0955	35.9118
7	0.0884	6.9630	23.5545	8.1285	25.3117	—	—	—	—	—
Overall	—	9.9381	24.8974	15.0994	30.8775	—	9.3516	23.5594	16.2542	30.9136
Group	Facebook					Skype-videochat				
1	0.4216	4.4201	20.7700	11.9557	32.7724	0.4216	4.3408	20.544	12.8354	33.2795
2	0.2862	8.4227	30.8524	14.4969	38.0183	0.4230	4.1481	20.9525	13.4634	33.9652
3	0.3862	6.0869	14.5694	13.3955	24.1807	0.3751	6.6947	15.6603	13.5717	24.4609
4	0.2097	8.5744	25.9577	14.0064	33.1636	0.5375	1.6203	7.4004	2.5731	10.9563
5	0.1263	12.514	27.2880	15.7297	30.9577	0.1824	8.4489	21.3063	9.7984	23.4784
6	0.1128	14.3447	34.1397	15.9733	35.8437	0.2256	6.0727	24.9642	6.4484	25.8884
7	0.2210	1.9788	10.5936	2.0172	10.7499	0.1179	4.9756	19.7093	6.4110	22.5335
Overall	—	5.7545	19.0159	8.8194	25.0937	—	5.3158	17.9998	9.0870	24.6192

Table 5: DC-DC converter tuning results of Patterns I and II.

Group	$W_{opt,I}$	$Gain_\eta$	$Gain_P$	$Gain_{\eta,max}$	$Gain_{P,max}$
1	0.2976	7.9717	29.7824	26.2208	40.8462
2	0.1886	14.047	38.7954	43.2898	46.5719
3	0.3751	6.4011	15.1687	13.8601	24.7137
4	0.1704	10.5933	29.3017	22.2939	39.5304
5	0.1263	12.8753	27.7511	17.7792	32.8968
6	0.1269	13.9486	33.7017	19.3969	38.6310
7	0.2137	2.0874	11.0332	6.8824	21.6813
Overall	—	6.2176	20.0263	13.6376	29.4715

Group	$W_{opt,II}$	$Gain_\eta$	$Gain_P$	$Gain_{\eta,max}$	$Gain_{P,max}$
1	0.3348	6.4977	26.7376	32.3645	39.9298
2	0.2115	6.1590	37.0320	33.1697	44.9638
3	0.3862	9.4790	14.7303	13.6770	24.4264
4	0.1835	12.4529	27.5864	22.0385	39.1593
5	0.1263	13.6757	27.2171	17.7792	32.8968
6	0.1269	2.0615	33.3899	19.3969	38.6310
7	0.2137	2.0874	10.9291	6.8824	21.6813
Overall	—	6.2955	20.0705	15.2870	30.0543

iv) *productivity* (contains 'Clock'), v) *system* (contains 'System setting'), vi) *games* (contains 'Neocore'), and vii) *maps* (contains 'GoogleMap'). We determine their run time according to the two types of usage patterns collected by i) deploying a custom logger on the phones of 33 Android users (Pattern I), ii) 222 Windows Mobile users across different demographics (Pattern II) in [15].

The current distribution from Pattern I is shown in Figure 4. The original power conversion efficiencies of Patterns I and II are 70.7410% and 70.4817%, respectively. Table 5 shows the optimization results for both Patterns I and II, where the values of W_{opt} are $W_{opt,I}$ for Pattern I, and $W_{opt,II}$ for Pattern II. The overall power conversion efficiency enhancements are from 6% to 15%, which correspond to from 20% to 30% power loss reduction during power conversion, respectively.

5. CONCLUSIONS

This paper demonstrated that significant power loss occurs during power conversion from the battery source to various devices in a modern smartphone. To mitigate this problem, the paper introduced a systematic method for system-level power conversion efficiency enhancement in smartphones. First, we proposed the equivalent power converter concept that abstracts the power conversion path from the battery to the modules into a single equivalent power converter. This enabled us to identify the model coefficients from application profiling. We demonstrated the accuracy of power conversion efficiency characterization and how the current power converter setup deviates from the optimal operating conditions. Finally, we proposed a power converter tuning procedure that resulted in 6% to 15% overall power conversion efficiency en-

hancement, which translates to up to 30% power loss reduction during power conversion. As part of the future work, the optimization procedure will be improved by considering a multitude of different applications and usage scenarios.

7. REFERENCES

[1] A. Shye, B. Scholbrock, and G. Memik, "Into the wild: Studying real user activity patterns to guide power optimizations for mobile architectures," *MICRO*, 2009.

[2] L. Zhang and et al., "Accurate online power estimation and automatic battery behavior based power model generation for smartphones," *CODES/ISSS*, 2010.

[3] M. Dong and L. Zhong, "Self-constructive high-rate system energy modeling for battery-powered mobile systems," *MobiSys*, 2011.

[4] A. Pathak, Y. C. Hu, M. Zhang, P. Bahl, and Y. Wang, "Fine-grained power modeling for smartphones using system call tracing," *EuroSys*, 2011.

[5] W. Yuan and K. Nahrstedt, "Energy-efficient soft real-time CPU scheduling for mobile multimedia systems," *SOSP*, 2003.

[6] D. Shin, Y. Kim, N. Chang, and M. Pedram, "Dynamic voltage scaling of oled displays," *DAC*, 2011.

[7] I. Choi, H. Shim, and N. Chang, "Low-power color TFT LCD display for hand-held embedded systems," *ISLPED*, 2002.

[8] Y. Choi, N. Chang, and T. Kim, "DC-DC converter-aware power management for low-power embedded systems," *IEEE T. on Computer-Aided Design of Integrated Circuits and Systems*, 2007.

[9] C. Shi, B. C. Walker, E. Zeisel, E. B. Hu, and G. H. McAllister, "A highly integrated power management IC for advanced mobile applications," *CICC*, 2006.

[10] B. Amelifard and M. Pedram, "Optimal design of the power-delivery network for multiple voltage-island system-on-chips," *IEEE T. on Computer-Aided Design of Integrated Circuits and Systems*, 2009.

[11] TexasInstruments, "Handset:smartphone," *http://www.ti.com/solution /handset_smartphone*.

[12] Qualcomm, "Snapdragon MDP MSM8660 datasheet," *https://devel oper.qualcomm.com/sites/default/files/snapdragon-mdp-8660.pdf*.

[13] J. Xiao, A. Peterchev, J. Zhang, and S. Sanders, "An ultra-low-power digitally-controlled buck converter IC for cellular phone applications," *APEC*, 2004.

[14] Y. Du, M. Wang, R. T. Meitl, S. Lukic, and A. Q. Huang, "High-frequency high-efficiency dc-dc converter for distributed energy storage modularization," *IECON*, 2010.

[15] F. Hossein, M. Ratul, K. Srikanth, L. Dimitrios, G. Ramesh, and E. Deborah, "Diversity in smartphone usage," *MobiSys*, 2010.